



Technological University Dublin  
ARROW@TU Dublin

---

Articles

Crest: Centre for Research in Engineering  
Surface Technology

---

2008

## A Highly Efficient Ag-ZnO Photocatalyst: Synthesis, Properties, and Mechanism

Suresh Pillai

*Technological University Dublin*, [suresh.pillai@tudublin.ie](mailto:suresh.pillai@tudublin.ie)

Michael Seery

*Technological University Dublin*, [michael.seery@tudublin.ie](mailto:michael.seery@tudublin.ie)

Reenamole Georgekutty

*Technological University Dublin*, [r.georgekutty@tudublin.ie](mailto:r.georgekutty@tudublin.ie)

Follow this and additional works at: <https://arrow.tudublin.ie/cenresart>

---

### Recommended Citation

Seery, M., Georgeknutty, R. & Pillai, S. C. (2008) A Highly Efficient Ag-ZnO Photocatalyst: Synthesis, Properties and Mechanism. *Journal of Physical Chemistry C*, vol. 112 no. 35, 2008, 13563-13570. doi:10.1021/jp802729a

This Article is brought to you for free and open access by the Crest: Centre for Research in Engineering Surface Technology at ARROW@TU Dublin. It has been accepted for inclusion in Articles by an authorized administrator of ARROW@TU Dublin. For more information, please contact [yvonne.desmond@tudublin.ie](mailto:yvonne.desmond@tudublin.ie), [arrow.admin@tudublin.ie](mailto:arrow.admin@tudublin.ie), [brian.widdis@tudublin.ie](mailto:brian.widdis@tudublin.ie).



This work is licensed under a [Creative Commons Attribution-Noncommercial-Share Alike 3.0 License](https://creativecommons.org/licenses/by-nc-sa/3.0/)



**Effect of Silver Modification on the Photocatalytic Activity of  
Nanocrystalline ZnO**

Journal:	<i>The Journal of Physical Chemistry</i>
Manuscript ID:	jp-2008-02729a.R1
Manuscript Type:	Article
Date Submitted by the Author:	n/a
Complete List of Authors:	Seery, Michael; Dublin Institute of Technology, School of Chemical and Pharmaceutical Sciences Georgekutty, Reenamole; Dublin Institute of Technology, School of Chemical and Pharmaceutical Sciences Pillai, Suresh; Dublin Institute of Technology, CREST



# A Highly Efficient Ag-ZnO Photocatalyst: Synthesis, Properties and Mechanism

*Reenamole Georgekutty,<sup>1,2</sup> Michael K. Seery,<sup>1\*</sup> Suresh C. Pillai,<sup>2\*</sup>*

<sup>1</sup>School of Chemical and Pharmaceutical Sciences, Dublin Institute of Technology, Kevin Street, Dublin  
8, Ireland.

<sup>2</sup>Centre for Research in Engineering Surface Technology (CREST), FOCAS Institute, Dublin Institute of  
Technology, Camden Row, Dublin 8, Ireland.

AUTHOR EMAIL ADDRESS (r.georgekutty@dit.ie, Michael.seery@dit.ie, suresh.pillai@dit.ie)

**RECEIVED DATE (to be automatically inserted after your manuscript is accepted if required  
according to the journal that you are submitting your paper to)**

TITLE RUNNING HEAD A Highly Efficient Ag-ZnO Photocatalyst

CORRESPONDING AUTHOR FOOTNOTE \* michael.seery@dit.ie, suresh.pillai@dit.ie

**ABSTRACT:** Highly photocatalytically active silver modified ZnO has been prepared and the effect of silver modification was studied. The structural and optical properties were characterised by XRD, FTIR, DSC, BET surface area, Raman, UV-Vis and photoluminescence spectroscopy. The photocatalytic activity of these materials was studied by analysing the degradation of an organic dye, rhodamine 6G (R6G), and it is found that 3 mol% silver modified ZnO at 400 °C shows approximately four times higher rate of degradation than that of unmodified ZnO and a three times higher rate than that of commercial TiO<sub>2</sub> photocatalyst standard Degussa P-25. It was also noted that the photocatalytic activity

1 for the modified ZnO sample was five times higher than the unmodified sample using sunlight. The  
2 effect of silver in enhancing the photocatalytic activity has been studied by analysing the emission  
3 properties of both ZnO and silver modified ZnO in the presence (emission increases) and absence  
4 (emission decreases) of R6G. We attribute these observations to the extent of valence band hole  
5 production and the role of silver in trapping the conduction band (CB) electrons in the absence of R6G.  
6 In the presence of R6G, the dye preserves the CB electron population in the metal oxide, thus preserving  
7 and enhancing emission intensity. The sensitizing property of the dye and electron scavenging ability of  
8 silver together constitute to the interfacial charge transfer process in such a way to utilise the  
9 photoexcited electrons.  
10  
11  
12  
13  
14  
15  
16  
17  
18  
19  
20  
21

22 **KEYWORDS;** ZnO, silver modification, visible-light photocatalysis, mechanism.  
23  
24

## 25 **1. Introduction**

26  
27 The application of semiconductors such as ZnO and TiO<sub>2</sub> in the area of photocatalysis has grown  
28 considerably, primarily because of their physical and chemical stability, high oxidative capacity, low  
29 cost and ease of availability.<sup>1,2,3,4,5,6</sup> Of the semiconducting materials, ZnO offers significant opportunity  
30 in providing electronic, photonic, and spin-based functionality (spintronics) because of its direct wide  
31 band gap (3.37 eV) and large exciton binding energy of ~60 meV. This makes it worthy in the potential  
32 and established hi-tech applications such as ceramics, piezoelectric transducers, optical coatings, high  
33 speed and display devices,<sup>7,8,9,10</sup> gas sensors,<sup>11</sup> varistors,<sup>12, 13</sup> photocatalysts<sup>14</sup> and photovoltaics.<sup>15</sup> Also  
34 the high chemical stability and low toxicity together make ZnO suitable for UV screening applications.  
35  
36  
37  
38  
39  
40  
41  
42  
43  
44  
45  
46

47 These semiconductors are well established and there has been considerable interest in their applications  
48 to the area of photocatalysis.<sup>16</sup> Because of their wide band gap, they absorb mainly in the UV region.  
49 Numerous studies report an improvement of visible-light photocatalytic activity of metal oxide  
50 semiconductors by doping with cations,<sup>17</sup> anions,<sup>18</sup> metals<sup>19</sup> and non-metals.<sup>20,21</sup> There are also some  
51 reports of the detrimental effect of dopants in the photocatalytic activity.<sup>22</sup> The photocatalytic activity of  
52 ZnO has been widely explored and reported.<sup>14,23</sup> In terms of studying the mechanism of photocatalysis,  
53  
54  
55  
56  
57  
58  
59  
60

1 ZnO offers some advantages over TiO<sub>2</sub>, primarily the fact that ZnO is quite strongly luminescent. This  
2 facilitates a study of the recombination of electron-hole pairs and hence a suitable probe in the study of  
3 highly active photocatalysts. The emission properties have also been used to sense the presence of  
4 organic molecules in its immediate vicinity.<sup>24</sup>  
5  
6  
7  
8  
9

10 The modification of semiconductors with noble metals has attracted significant attention especially in  
11 heterogeneous photocatalysis.<sup>25,26</sup> Incorporating silver in ZnO is now an exciting area in research for  
12 developing electronic applications. In addition, silver modification is found to be effective for the  
13 fabrication of *p*-type ZnO,<sup>27</sup> as the naturally occurring ZnO displays *n*-type conductivity due to its  
14 native defects such as zinc interstitials and oxygen vacancies. The modification with silver has  
15 influenced the photocatalytic activity of nanocrystalline photocatalysts because of its optical and  
16 electronic properties.<sup>28,29,30</sup> In our previous study, we reported a significant enhancement in  
17 photocatalytic activity of TiO<sub>2</sub> by modification with silver.<sup>31</sup> Recently, Kamat and co-workers have  
18 studied the interfacial electron transfer process in silver modified TiO<sub>2</sub>.<sup>32</sup> Extensive research is  
19 underway to depict the exact role of silver in increasing the visible light response of metal oxides. Silver  
20 can trap the photogenerated electrons from semiconductor and allow the holes to form hydroxyl radicals  
21 which results in the degradation reaction of organic species present. Moreover, silver can enhance the  
22 photocatalytic activity by creating a local electric field and the optical vibration of surface plasmon in  
23 silver can make a reasonable enhancement in this electric field.<sup>30</sup> The increased photocatalytic activity of  
24 silver modified ZnO is reportedly due to the change in the surface properties such as oxygen vacancies  
25 and crystal defects.<sup>33</sup>  
26  
27  
28  
29  
30  
31  
32  
33  
34  
35  
36  
37  
38  
39  
40  
41  
42  
43  
44  
45  
46  
47

48 Although there are reports about the effect of silver addition in the electric and optical properties of ZnO  
49 for electronic applications,<sup>34</sup> to the best of our knowledge, there are no detailed studies on the effect of  
50 silver modification in ZnO based on various calcination temperatures.<sup>35</sup> In this paper, we report a  
51 systematic study on the effect of silver modification in ZnO and consequent photocatalytic activity. The  
52 methodology of synthesis of our materials reported here is through a straight-forward non-aqueous  
53  
54  
55  
56  
57  
58  
59  
60

1 route. The enhancement in photocatalytic activity due to the presence of silver is studied by  
2 characterisation of the materials and optimisation of the reaction conditions. A possible mechanism of  
3 photocatalysis is also been presented by analysing the effect of various amounts of silver in the emission  
4 properties of both ZnO and Rhodamine 6G dye.  
5  
6  
7  
8

## 9 10 **2. Experimental section**

### 11 **2.1 Materials**

12  
13 Zinc acetate dihydrate (98%), oxalic acid (97%), silver nitrate (99%) and ethanol were purchased from  
14 Aldrich and used as received. The dye used for the photocatalytic study (rhodamine 6G) was purchased  
15 from Eastman and was of analytical reagent grade and used without further purification. Double distilled  
16 water was used in all the experiments.  
17  
18  
19  
20  
21  
22  
23

24  
25 **2.2 Preparation of ZnO powders:** In a typical experiment, zinc acetate (10.98 g, 50 mM) was  
26 dissolved in ethanol (500 mL) at 60 °C and stirred for 30 min. Oxalic acid (12.55 g, 100 mM) dissolved  
27 in ethanol (200 mL) at 60 °C was slowly added to the warm ethanolic solution of zinc acetate. The  
28 mixture was stirred for 2 h. The thick white colloidal semi-gel formed was allowed to dry at 80 °C  
29 overnight. The dried xerogel was further calcined at different temperatures (300 °C – 1000 °C) for 2 h to  
30 get ZnO powder.  
31  
32  
33  
34  
35  
36  
37  
38  
39

40 For silver modified ZnO, various mol% (1, 3, 5 and 10) of silver nitrate dissolved in ethanol were added  
41 to the zinc acetate-oxalic acid solution above, with stirring. This was dried as above and calcined at  
42 different temperatures for 2h.  
43  
44  
45  
46  
47

### 48 **2.3 Characterisation**

49  
50 The crystallinity and the effect of silver modification in the crystal phases of the synthesised ZnO and  
51 silver modified ZnO powders were characterised by X-ray diffraction technique with a Siemens D 500  
52 X-ray diffractometer in the diffraction angle range  $2\theta = 20-70^\circ$ , using Cu  $K_\alpha$  radiation. The crystallite  
53 size D of the samples were estimated using the Scherrer's equation,  $(0.9\lambda)/(\beta\cos\theta)$ , by measuring the  
54  
55  
56  
57  
58  
59  
60

1 line broadening of (101) main intensity peak, where  $\lambda$  is the wavelength of  $\text{CuK}\alpha$  radiation,  $\beta$  is the full  
2 width at half maximum and  $\theta$  is the Bragg's angle.  
3  
4

5 Differential Scanning Calorimetry (DSC) measurements were carried out to examine the phase changes  
6 using a Rheometric Scientific DSC QC. About 6 mg of the dried sample was heated from room  
7 temperature (25 °C to 500 °C at a constant heating rate of 10 °C/min. The formation of ZnO was  
8 confirmed by measuring the FTIR spectra of ZnO and silver modified ZnO samples using a GX-FTIR  
9 spectrophotometer. In order to study the optical properties, the diffuse reflectance and absorbance  
10 spectra of samples were measured using a UV-VIS-NIR Perkin Elmer spectrophotometer. Room  
11 temperature photoluminescence spectra of the prepared samples were obtained from Perkin Elmer  
12 Luminescence Spectrometer (LS50B). The excitation wavelength was 325 nm, and spectra (uncorrected)  
13 were obtained in the range 350 nm to 600 nm.  
14  
15  
16  
17  
18  
19  
20  
21  
22  
23  
24  
25  
26

## 27 **2.4 Photocatalytic studies**

28 For photocatalytic activity studies,  $0.06 \pm 0.005$  g of powdered sample was dispersed in 50 mL of  
29 aqueous rhodamine solution having concentration  $5 \times 10^{-6}$  M at pH ~6. The dispersion was irradiated by  
30 light using Q-Sun solar simulator ( $0.68 \text{ W/cm}^2$  at wavelength 340 nm) with stirring. Aliquots were  
31 collected at various time intervals to monitor the degradation of rhodamine. Samples were centrifuged  
32 and the absorption spectra were measured. The rate constant for degradation was obtained from a first  
33 order plot.  
34  
35  
36  
37  
38  
39  
40  
41  
42  
43  
44  
45

## 46 **3. Results**

### 47 **3.1 Characterisation of Materials**

48 The powder X-ray diffraction patterns of unmodified and various mol% of silver modified ZnO samples  
49 calcined at 300 and 400 °C are shown in Figure 1. The XRD pattern of 300 °C calcined samples show  
50 peaks corresponding to zinc oxalate dihydrate and the Ag modified ZnO samples show peaks  
51 corresponding to  $\text{Ag}_2\text{O}$  in addition to anhydrous zinc oxalate precursors.<sup>36</sup> Conversely, the spectra of  
52  
53  
54  
55  
56  
57  
58  
59  
60

400 °C samples show typical peak patterns of ZnO wurtzite structure (JCPDS, 36-1451) and the characteristic peaks of metallic silver.<sup>12,31</sup>

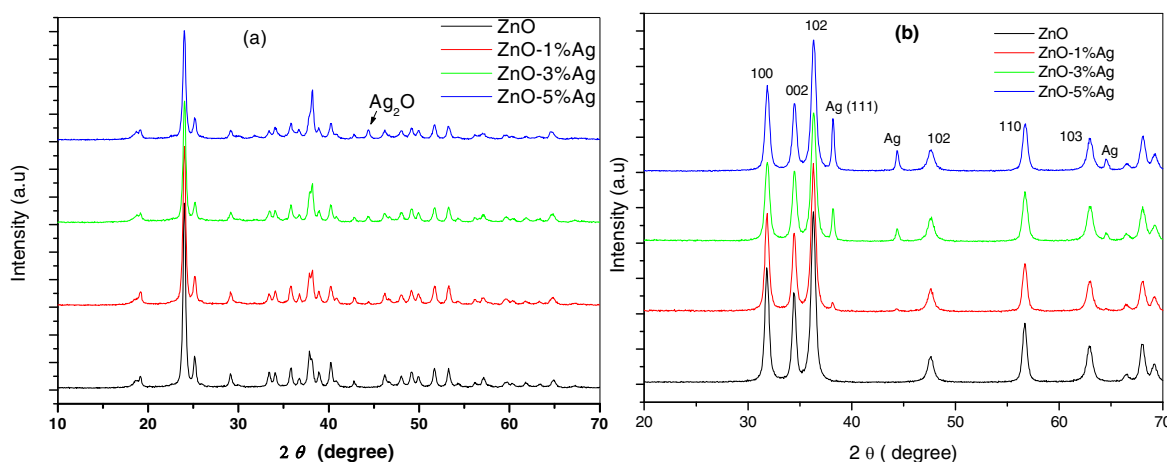


**Figure 1:** Powder XRD patterns of ZnO and various mol % of Ag modified ZnO samples calcined at (a) 300 °C and (b) 400 °C.

Furthermore, a consistent increase in the intensity of silver peaks can be noted with the increase in concentration of Ag from 1 to 5 mol%. It should be noted that the formation of metallic silver and the crystalline phase of ZnO is starting at above 300 °C. This is consistent with the thermal decomposition behaviour of zinc oxalate precursors and Ag<sub>2</sub>O systems.<sup>36, 37</sup> The result also corresponds with a recent observation by Ahn *et al* who studied the thermal decomposition of Ag<sub>2</sub>O in ZnO system.<sup>38</sup> Therefore, we believe that in the present ZnO system, Ag<sub>2</sub>O is the stable phase at 300 °C and as the temperature increases to 400 °C, Ag<sub>2</sub>O decomposes to metallic silver. According to some previous reports, Ag can be incorporated in ZnO system either as a substituent for Zn<sup>2+</sup> or as an interstitial atom.<sup>39,40</sup> If the silver is substituted for Zn<sup>2+</sup>, a corresponding peak shift would be expected in the XRD. No such shift in the peak positions was observed in any of our modified samples. This indicates the segregation of Ag particles in the grain boundaries of ZnO crystallites rather than going into the lattice of ZnO, or only an insignificant quantity may be going to the substitutional Zn site.



The crystallite sizes of unmodified ZnO and various mol% of Ag modified ZnO samples calcined at different temperatures were calculated from the X-ray line broadening using the Scherrer equation. (Supporting Information 1). It is clear that the addition of silver causes a slight reduction in crystallite size. In general, the crystallite size of all the samples increases with increasing calcination temperature (Figure 2), whereas silver facilitates the densification of particles at high temperatures.

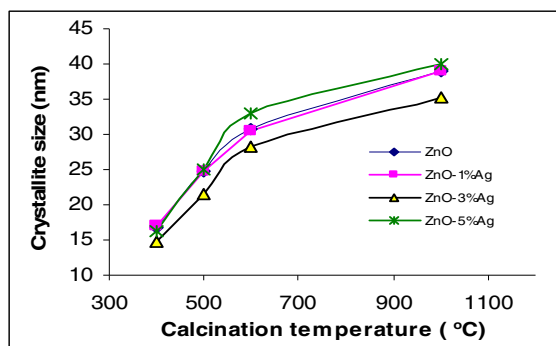


**Figure 2:** Plot of crystallite size Vs calcination temperature.

In order to understand the thermal events in the samples, DSC has been performed. The DSC curves of ZnO and Ag modified ZnO (AZ) samples are shown in Figure 3. The unmodified ZnO shows three endothermic peaks starting at 68, 104 and 405 °C. On the other hand, 3 mol% Ag modified ZnO shows two endothermic peaks at 68, 112 °C and two exothermic peaks at 183 and 395 °C respectively. The endothermic peak at ~68 °C corresponds to the elimination of ethanol and the one at ~104 °C may be attributed to the removal of structural water. The endothermic peak at 405 °C represents the removal of oxalate species.<sup>41</sup>

In comparison, the exothermic peak observed at 184 °C for the Ag modified ZnO is assumed to be the formation of Ag<sub>2</sub>O where as Ag<sup>+</sup> is stable in the form of AgO<sub>x</sub> or Ag<sub>2</sub>O at these temperatures.<sup>42</sup> Interestingly, an intense exothermic peak at 390 °C shows the thermal decomposition of Ag<sub>2</sub>O to metallic silver, which is in the same temperature region where an endothermic peak is observed for unmodified ZnO; the latter representing the formation of ZnO at this temperature. This is in good agreement with XRD results and is consistent with a previous report.<sup>38</sup> The exothermic formation of

metallic silver is highly energetically favourable than the endothermic evolution of ZnO. In other words, the highly exothermic nature of metal formation predominates in DSC compared to endothermic ZnO formation. In addition, an increase in silver concentration shows an increase in this peak intensity, which confirms this assumption.

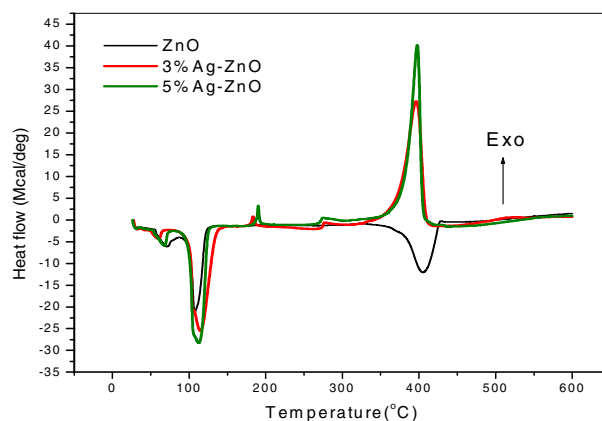


**Figure 3:** DSC of unmodified ZnO and Ag modified ZnO samples

The formation of nanocrystalline ZnO wurtzite structure and the effect of silver addition in ZnO were further confirmed by FT-IR spectral analysis, which is shown in Figure 4. The spectrum of as prepared ZnO prior to calcination shows an absorption peak at  $\sim 3400\text{ cm}^{-1}$  which corresponds to the O-H stretching of surface adsorbed water molecule. The band at  $\sim 2900\text{ cm}^{-1}$  shows the presence of C-H species. The three bands occurring in the region of  $1000 - 500\text{ cm}^{-1}$  and the one at  $1380\text{ cm}^{-1}$  correspond to the different modes of  $\text{CO}_3^{2-}$ .

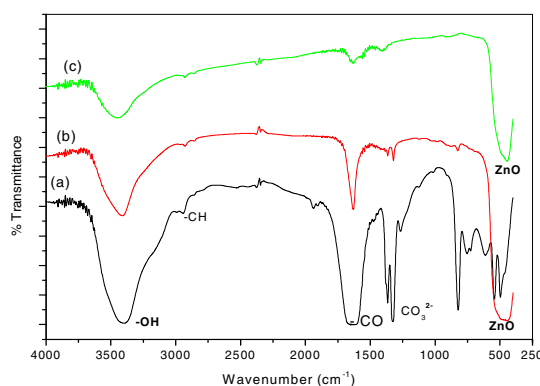


**Figure 4:** FTIR spectra of ZnO (a) as prepared at 80 °C, (b) calcined at 400 °C and (c) 3 mol% Ag modified ZnO calcined at 400 °C.

Further the symmetric and asymmetric stretching bands of acetate species can be observed at 1360 and 1600  $\text{cm}^{-1}$ .<sup>17</sup> All of these indicate that the zinc acetate precursors are present. However, in the case of ZnO at 400 °C, the peaks corresponding to the organic precursor are no longer present and show the peak of only nanosized ZnO at  $\sim 490 \text{ cm}^{-1}$ . The silver modified ZnO at 400 °C as well as the IR spectra at 300 °C, however, (Supporting Information 2) show no bands for silver, only that of ZnO, indicating there is no chemical bonding between silver and ZnO.

In order to assess the crystal quality or the amount of defects, Raman analysis has been carried out on the samples. Raman spectra of ZnO and silver modified ZnO at 400 °C are shown in Figure 5. The most intense peak at  $436 \text{ cm}^{-1}$  corresponds to  $E_2$  mode of ZnO hexagonal wurtzite structure and one at  $326 \text{ cm}^{-1}$  should be assigned as the second order Raman spectrum arising from the zone boundary phonons  $3E_{2H} - E_{2L}$ , while a smaller shoulder at  $574 \text{ cm}^{-1}$  is the contribution from  $E_1(\text{LO})$  mode associated with oxygen deficiency.<sup>43</sup> A stronger  $E_2$  mode and much lower  $E_1$  mode indicate its good crystal quality, with only a very low oxygen vacancy. On the other hand, in addition to the ZnO peaks the silver modified ZnO shows a weak peak at  $560 \text{ cm}^{-1}$  followed by the peak corresponding to oxygen deficiency.

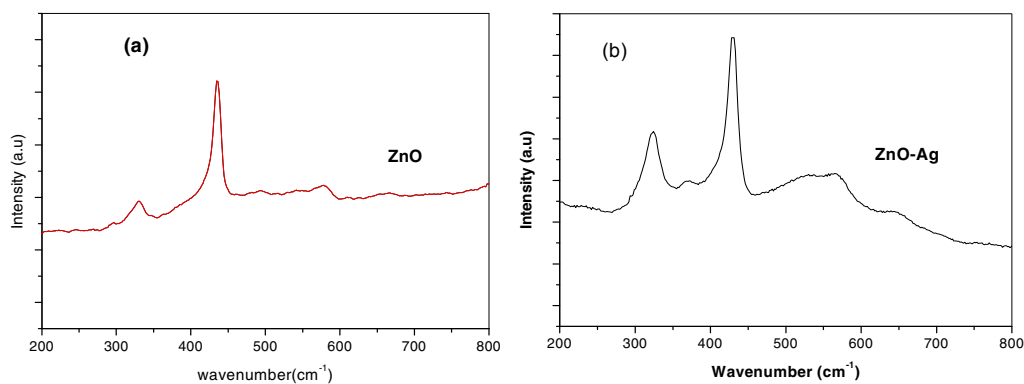


**Figure 5:** Raman spectra of ZnO and silver modified ZnO at 400 °C.

The absorption spectra of unmodified and silver modified ZnO are presented in Figure 6 and it can be seen that the silver addition does not make any significant reduction in its band gap.

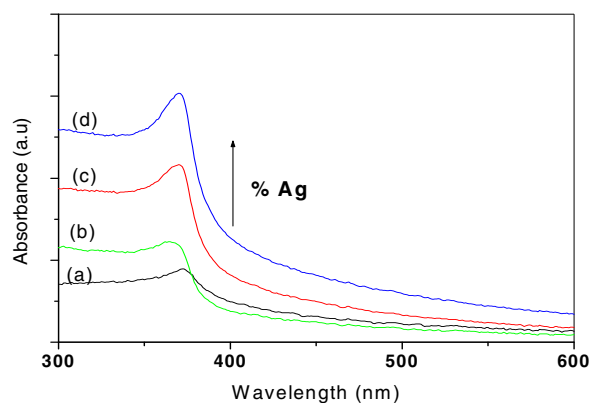
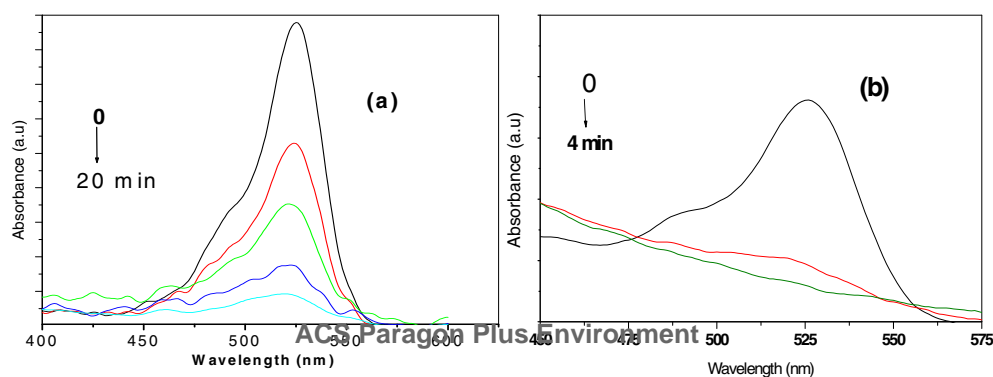


**Figure 6:** UV-visible absorption spectra of ZnO (a) and (1-5) mol% silver modified ZnO at 400 °C

### 3.2 Photocatalytic Activity

An important aim of the study involves the examination of photocatalytic activity of ZnO and various mol% of silver modified ZnO at different temperatures. The use of an aromatic compound rhodamine 6G (R6G) as a model dye for the photocatalysis study is mainly due to their recurrent occurrence in the industrial field.<sup>44,45</sup> The photocatalytic activity of unmodified and various mol% of silver modified ZnO powders at temperatures ranging from 300 – 1000 °C have been studied by analysing the degradation of the dye. The absorption spectra of R6G after undergoing photocatalytic degradation by unmodified and silver modified ZnO at 400 °C are shown in Figure 7. The degradation is monitored by studying the decrease in absorbance of R6G in presence of powdered sample suspensions, and quantified by plotting a first order decay plot of the absorbance at 525 nm.



1  
2  
3  
4  
5  
6  
7 **Figure 7:** UV-visible absorption spectra of degradation of R6G by (a) ZnO and (b) 3 mol% silver  
8 modified ZnO at 400 °C  
9

10  
11  
12 In the case of metal modification in nanoparticles, a particular concentration of metal modifier can tune  
13 the photophysical properties. From the study, it can be seen that the addition of silver enhances the  
14 photocatalytic degradation of the dye up to 3 mol% and above this concentration it shows a decrease in  
15 the rate of activity. The higher percentage of silver could be unfavourable to photocatalytic efficiency. It  
16 is assumed that amount of silver below its optimum, can act as electron-hole separation centres.<sup>46</sup> When  
17 the Ag loading above its optimum, it can also act as charge carrier recombination centres. This is  
18 because the possibility of hole capture increases by large number of negatively charged Ag particle on  
19 ZnO which reduces the efficiency of charge separation when the silver content is above its optimum.<sup>47</sup>  
20  
21  
22  
23  
24  
25  
26  
27  
28  
29  
30  
31  
32  
33

34 Hence, in the present system, the optimum amount of silver giving the highest photocatalytic activity  
35 (Figure 8) is determined to be 3 mol% whose rate of degradation is four times greater ( $0.42 \text{ min}^{-1}$ ,  
36 degrade the dye within 4 min) compared to the rate with pure ZnO ( $0.10 \text{ min}^{-1}$ , degrade the dye within  
37 20 min). The samples at 400 °C show a better photocatalytic activity than the samples at higher  
38 temperatures, which may be attributed to the smaller crystallite size and a reasonably good surface area.  
39 (Supporting Information 1). The surface area analysis of ZnO ( $32 \text{ m}^2/\text{g}$ ) and 3% silver modified ZnO(  
40  $173 \text{ m}^2/\text{g}$ ) at this temperature shows good agreement with this activity. It should be noted that the Ag  
41 modified samples (3 and 5 mol%) showed almost similar rate of photocatalytic activity at higher  
42 temperatures such as 400 – 600 °C and hence 3 mol% silver is found to be as the optimum  
43 concentration.  
44  
45  
46  
47  
48  
49  
50  
51  
52  
53  
54  
55  
56  
57  
58  
59  
60

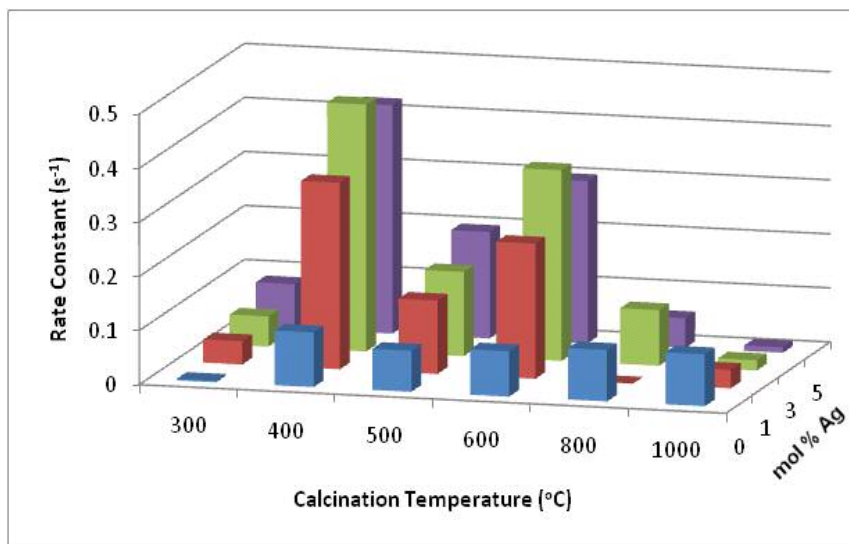


**Figure 8:** Plot of concentration of silver vs. rate constants of degradation reaction obtained from kinetic analysis.

Nevertheless, at higher temperatures, it is found that there is no positive effect of silver addition in the photocatalytic activity (800 – 1000 °C) (Supporting Information 3). On the other hand, the silver modification is photocatalytically effective only at low temperatures. This is because the presence of silver promotes the densification and grain growth of ZnO at high temperatures<sup>48</sup> by forming silver island in the ZnO matrix, which causes the reduction in active surface sites of the photocatalyst for the adsorption of degradants and for the absorption of light. This conclusion has been further confirmed by BET analysis of high temperature (800 °C) calcined sample which shows a lower surface area and pore volume for silver modified ZnO (2.65 m<sup>2</sup>/g, 0.005 cc/g) than the pure ZnO (4.34 m<sup>2</sup>/g, 0.012 cc/g). The crystallite size of 3 mol% Ag modified sample showed the smallest size values among the samples and had good photocatalytic activity. 3 mol% may therefore be assumed as the optimum concentration of Ag particles for the present ZnO system. This is similar to previous findings for silver loading in titania materials<sup>31</sup> and to other work involving cobalt on cobalt oxide/titania systems.<sup>49</sup>

Although there is no formation of ZnO at 300 °C, the silver modification causes the zinc oxalate precursor at 300 °C to show improved photocatalytic activity. This may be due to the fact that Ag<sub>2</sub>O is

1 present in the system, which is also a metal oxide, and can produce holes on light illumination resulting  
2 in hydroxyl radicals which subsequently degrade the dye.<sup>50</sup>  
3

4  
5 The visible light activity of these materials has also been analysed in presence of Dublin sunlight and it  
6 is found that silver modified ZnO shows 5 times higher rate of degradation of the dye than the pure ZnO  
7 (Supporting Information 4) which is an indication that these silver modified materials could be utilised  
8 for sunlight driven photocatalytic processes.  
9  
10  
11  
12  
13  
14  
15  
16

### 17 3.3 Photoluminescence Studies

18  
19 Photoluminescence (PL) studies give an insight into the optical and photochemical properties of ZnO.  
20 Information on the quality of crystals, structural defects (surface oxygen vacancies, Zn interstitials *etc*)  
21 and particle surfaces can be garnered from PL spectra. The room temperature PL emission spectra  
22 (excitation at 325 nm) of ZnO and various mole % of Ag modified ZnO samples calcined at 400 °C are  
23 shown in Figure 9. All samples emit strongly in the UV with a band centred at 390 nm, corresponding to  
24 the excitonic emission and three other less intense peaks. The weak blue band at 421 nm and 480 nm  
25 correspond to band edge free excitons and bound excitons respectively.<sup>51</sup> Furthermore, there is a weak  
26 green emission at 530 nm. The exact reason for this green emission is still controversial. A number of  
27 hypotheses have been proposed to explain this such as transition between electron close to the  
28 conduction band and a deeply trapped hole at  $V_o^{++}$ , surface defects like  $Zn^{2+}$  vacancies, due to the  
29 transition between anti-site oxygen and donor-acceptor complexes,<sup>52</sup> *etc*. Surface binding of carboxylate  
30 ions is also known to improve the emission yield as they create vacancies that can facilitate the visible  
31 emission.<sup>53</sup>  
32  
33  
34  
35  
36  
37  
38  
39  
40  
41  
42  
43  
44  
45  
46  
47  
48  
49  
50  
51  
52  
53  
54  
55  
56  
57  
58  
59  
60

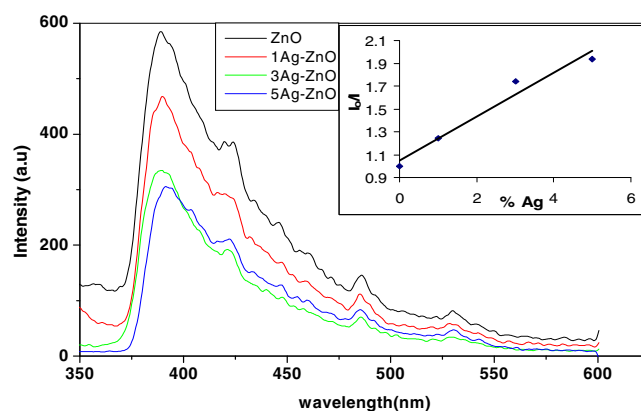


**Figure 9:** Room temperature PL spectra of ZnO and various mole % of Ag modified ZnO samples calcined at 400 °C. (Excitation at 325 nm). Inset shows the relative intensity change of emission in presence of silver. Emission intensities were measured at 390 nm.

According to some reports, this longer wavelength emission is due to the recombination of photogenerated hole with the singly ionized oxygen vacancy site.<sup>54,55</sup> Our study agrees with this report as the presence of oxygen vacancies is also confirmed from the Raman analysis. The weak green emission and strong exciton emission of the materials demonstrate its good crystal quality.

Also it could be seen from the PL spectra that, the UV emission is decreasing with an increase in silver content indicating the decreased electron-hole recombination. This decrease in emission intensity is in accordance with the Stern- Volmer quenching and similar results were previously reported.<sup>56</sup>

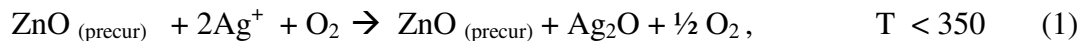
## 4. Discussion

### 4.1 Effect of Synthetic Parameters on Photocatalytic Activity

A non-aqueous sol-gel process adopted for the present study helps Ag particles to disperse well in the ZnO matrix. Such a distribution is observed to be favouring the tuning of structural features for achieving better photocatalytic activity, which was found to be better (three times) than the commercial photocatalyst, Degussa P25. The silver modified samples at 400 °C are found to be highly photoactive, with nanocrystalline ZnO formed at this temperature. The formation of nanocrystalline ZnO at 400 °C was also reported by Wang *et al*<sup>57</sup> where crystalline ZnO nanowires in presence of gold were observed. The segregation of metallic Ag particles around the highly crystalline ZnO grain boundaries may be the



1 reason for the high photocatalytic activity of the 400 °C calcined samples. The incorporation of silver  
2 can be represented according to Scheme (1).  
3  
4



10 Like monovalent dopant such as  $\text{K}^+$ ,  $\text{Na}^+$ , silver can perform as amphoteric dopant according to scheme  
11 (2), where  $\text{Ag}_{(\text{Zn})}$  is the silver occupied in the Zn site and  $\text{Ag}_{(i)}$  is the Ag in the interstitial site.  
12  
13  
14  
15  
16



20 In the present case, the presence of Ag in the ZnO lattice is ruled out given the absence of a shift in the  
21 X-ray peak position. Because of the difference in ionic radii between  $\text{Ag}^+$  (1.22 Å) and  $\text{Zn}^{2+}$  (0.72 Å),  
22 the silver particles preferentially choose to segregate around the ZnO grain boundaries. It is also  
23 observed from XRD that metallic Ag particles are formed only at 400 °C. Indeed, the 300 °C samples  
24 show the X-ray reflections corresponding to zinc acetate precursor and  $\text{Ag}_2\text{O}$ . This observation  
25 corroborates with previous reports, where the thermal decomposition behaviour of ZnO precursors was  
26 studied.<sup>12</sup> Also it has been reported that the thermal decomposition of  $\text{AgO}_x$  into Ag occurs in the  
27 temperature range 350 - 400 °C.<sup>58,59</sup> Our observations are similar to this study and to the other reports  
28 which describe the thermal stability of chemically precipitated  $\text{Ag}_2\text{O}$  powders.<sup>60,61</sup>  
29  
30  
31  
32  
33  
34  
35  
36  
37  
38  
39  
40  
41  
42

43 Ahn *et al* have also studied the thermal decomposition of  $\text{Ag}_2\text{O}$  in ZnO system, where they reported that  
44 the thermal decomposition of  $\text{Ag}_2\text{O}$  to metallic silver occurs above 380 °C.<sup>38</sup> These findings are in good  
45 agreement with the DSC result, where the crystallization of ZnO as well as the decomposition of  $\text{Ag}_2\text{O}$   
46 occurs above 380 °C. It is also evident from XRD that the incorporation of Ag into the ZnO matrix does  
47 not make considerable change in the crystalline growth of nano ZnO compared to unmodified ZnO.  
48 However, the incorporation of 3 mol% Ag at 400 °C was found to be inhibiting the temperature  
49 dependent crystal growth of ZnO. Therefore, 3 mol% can be assumed as the optimum concentration of  
50 Ag particles required for the effective homogeneous distribution in the ZnO matrix by which the  
51  
52  
53  
54  
55  
56  
57  
58  
59  
60

1  
2  
3  
4  
5  
6  
7  
8  
9  
10  
11  
12  
13  
14  
15  
16  
17  
18  
19  
20  
21  
22  
23  
24  
25  
26  
27  
28  
29  
30  
31  
32  
33  
34  
35  
36  
37  
38  
39  
40  
41  
42  
43  
44  
45  
46  
47  
48  
49  
50  
51  
52  
53  
54  
55  
56  
57  
58  
59  
60

properties can be tuned effectively. On increasing concentration, the Ag particles can aggregate together and form localized clusters, which reduce the possibility of a homogeneous distribution and thereby reduce the surface availability for the adsorption of reactant and light.

Moreover, at high temperatures, since the Ag-O bond strength is weaker than the Ag-Ag bond strength, the formed Ag<sup>0</sup> has higher surface energy eventually will form metallic clusters, which facilitate the densification of ZnO which reduces the surface area and hence the photocatalytic activity. The photocatalytic activity is dependent on the exposed surface area of the photocatalyst as it provides a means for the surface adsorption of the degradant. These results appear consistent with studies of Dodd *et al*<sup>62</sup> who reported that there exists an optimum particle size for maximum photocatalytic activity of ZnO. This optimum particle size of ~15 nm, in the present study, was achieved by the suitable amount of silver addition. It is evident from the crystallite size (Figure 2) that 3 mol% silver modified ZnO at 400 °C shows a smaller crystalline size among other samples. The distribution of silver in the ZnO matrix resulted in a reduction in the crystallite size. In a particular system, a smaller particle size, which causes the specific surface area to increase, is expected to enhance the surface active sites where the photogenerated charge carriers are able to react with surface adsorbed molecule to form active radicals. High crystallinity with a low particle size results in a reasonable surface area for enhanced photocatalytic activity.

As well as surface modification, it is evident from the absorption spectra that the silver addition can enhance the absorption capability of ZnO. Even though there is no considerable change in the band gap (calculated from diffuse reflectance spectra), the energy levels of silver lying in between the VB and CB of ZnO may facilitate the enhanced light absorption capability.

## 4.2 Mechanism of Enhancement of Photocatalytic Activity by Silver

One of the major aims behind the modification of semiconductors with noble metals is to improve or tune the catalytic and sensing properties. The deposition of noble metals on semiconductor nanoparticles is an effective way for improving the photocatalytic efficiency as the metal modifier can indirectly influence the interfacial charge transfer processes. As a noble metal, silver can act as electron scavenger and store them effectively. Certainly, a primary understanding of photoinduced interactions as well as the interfacial charge transfer processes in metal modified semiconductors is important to explain the exact role of metal in semiconductor photocatalysis. Light absorption of a suitable wavelength by ZnO results in the promotion of an electron from the valence band to the conduction band. The resulting hole is primarily responsible for the formation of hydroxyl radicals, which subsequently degrade the pollutants adsorbed onto the surface of the photocatalyst.<sup>63</sup> In such a photocatalytic process, the separation and recombination of photoinduced charge carriers are competitive pathways and photocatalytic activity is effective when recombination between them is prevented. The extent of recombination can be gauged by the intensity of luminescence.

In the present case, the UV emission at 390 nm of ZnO reduces as a function of mol % of silver (Figure 9). This gradual decrease can be ascribed to the electron trapping effect of Ag, which acts as an acceptor species, hindering the recombination of charge carriers on ZnO.<sup>64</sup> Similar results were found with titanium dioxide.<sup>65</sup> The Fermi level of silver, which lies below the conduction band of ZnO, energetically favours the transfer of electrons from ZnO. In order to assess the nature of photocatalytic degradation of R6G, we analysed the emission spectra of ZnO and silver modified ZnO in presence of R6G which is shown in Figure 10.

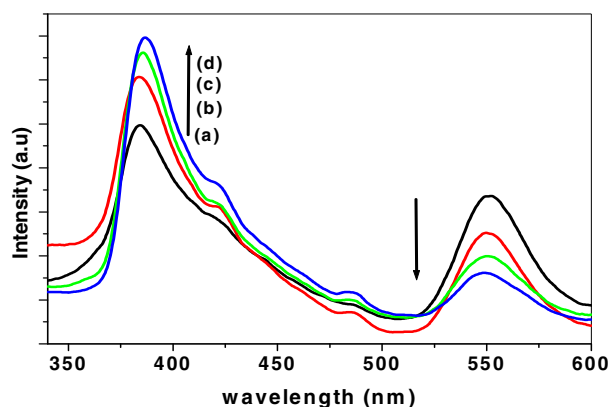


**Figure 10:** Room temperature PL spectra of (a) ZnO and (b), (c), (d) are 1, 3 & 5 mol% Ag modified ZnO respectively in presence of R6G. Emission at 390nm corresponds to ZnO emission and at ~550nm corresponds to R6G.

An increase in intensity of UV emission (390 nm) of ZnO, as a function of amount in silver was observed, which is reverse in the case of samples without R6G. Interestingly, this increase in ZnO emission coincides with the decrease in emission of R6G at ~550 nm indicating that there is an additional photoelectrochemical process that dominates the electron capturing by silver at the time of photodegradation of R6G. These findings indicate the degradation of R6G on the silver modified ZnO surfaces may occur by a simultaneous two stage charge transfer processes.

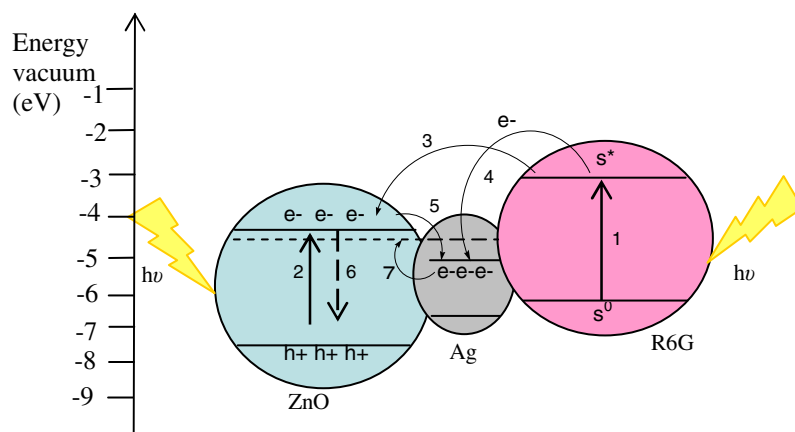


**Figure. 11:** Schematic showing the electron transfer events of Ag-ZnO system in presence of R6G. (1)  $S^0$  to  $S^*$ ; (2) VB to CB in ZnO (charge carrier generation); (3)  $S^*$  to CB of ZnO; (4)  $S^*$  to Ag; (5) CB of ZnO to Ag and (6) CB to VB of ZnO (charge carrier recombination) (7) Shifting of Fermi level of silver.

1 The high reduction potential of S\*, CB of ZnO (-0.8 V Vs NHE) and of Ag (0.15V) (according to  
2 literature data)<sup>66, 67</sup> drives its electron injection reactions.  
3  
4  
5

6 The possible interfacial charge transfer events in the silver modified semiconductor at the time of  
7 degradation of dye can be explained by using the diagram presented in Figure 11. After the initial  
8 events such as the (1) ground state singlet to singlet excitation in dye and (2) band-gap excitation in  
9 ZnO, the possible electron transfer processes that can happen in the Ag-ZnO system in photocatalytic  
10 degradation of R6G are transfer of electrons from (3) sensitized dye to the conduction band of ZnO, (4)  
11 sensitized dye to Ag particles, (5) from the CB of ZnO to Ag, (6) from the CB of ZnO to its VB  
12 (recombination) and sensitized dye to the shallow trap levels in the band gap of ZnO. From the UV-vis  
13 and PL spectra it is found that an increase of Ag concentration in the system enhances the UV emission  
14 of ZnO in presence of R6G, while diminishes in the absence of dye. This could be ascribed to the extent  
15 of hole formation as a function of Ag concentration.<sup>68</sup> The greater the formation of holes, the more  
16 intense the UV emission, provided all charge carriers are recombining effectively. However, in the  
17 absence of R6G, the CB electrons of ZnO generated as a result of the band-gap excitation are captured  
18 by the Ag particles and the recombination is reduced significantly; hence we observe a decrease in  
19 emission intensity as the Ag concentration increases. Further, an increase in the hole concentration  
20 formed as a function of Ag addition also found to enhance the UV emission by a similar mechanism. In  
21 presence of R6G, however, the CB electron population in ZnO is retained by the electron injection from  
22 the dye, which also simultaneously populates the electron level in Ag. Both processes (4) and (5) are  
23 possible in the case of silver because of the position of its energy level.<sup>69</sup> This electron transfer will  
24 continue until the overall Fermi level of the metal modified ZnO system shifts towards more negative  
25 potential (7) and ultimately equilibrates with that of ZnO.<sup>70</sup> Once this level is reached, Ag discharges  
26 the stored electrons in to the solution where they react with dissolved oxygen to form the superoxides  
27 and OH radicals in turn. These active oxygen species react with the dye molecules and degrade them  
28 effectively.  
29  
30  
31  
32  
33  
34  
35  
36  
37  
38  
39  
40  
41  
42  
43  
44  
45  
46  
47  
48  
49  
50  
51  
52  
53  
54  
55  
56  
57  
58  
59  
60

1  
2  
3  
4  
5  
6  
7  
8  
9  
10  
11  
12  
13  
14  
15  
16  
17  
18  
19  
20  
21  
22  
23  
24  
25  
26  
27  
28  
29  
30  
31  
32  
33  
34  
35  
36  
37  
38  
39  
40  
41  
42  
43  
44  
45  
46  
47  
48  
49  
50  
51  
52  
53  
54  
55  
56  
57  
58  
59  
60

If there was back electron transfer between the excited dye cation radical ( $\text{dye}^{+\bullet}$ ) and ZnO ( $e^-$ ), the dye would have regenerated. However, no dye regeneration was observed which indicates suppression of this back electron transfer by silver. Hence, there is a role for silver in utilising the captured electrons and thereby the free holes in the case of a system containing sensitizing dye. The enhanced photocatalytic activity of semiconductors modified with Ag are previously reported to be due to the generation of more free VB holes as a function of silver addition. However, in the present case, active oxygen species such as OH radicals and  $\text{O}_2^{\bullet-}$  generated by the CB electrons are found to be major species responsible for the dye degradation. Both the sensitizing property of dye and electron scavenging ability of silver together constitute to the interfacial charge transfer process in such a way to utilise the photoexcited electrons, in addition to the VB holes, to form this active oxygen species. The high reduction potential of the dye used is found to be the key factor that governs the electron transfer process and thereby defines the mechanism of photocatalytic degradation.

## 5. Conclusions

Various mol% of highly active silver modified and unmodified ZnO photocatalysts at different temperatures were prepared through a non aqueous sol gel route. The structural and optical properties of the resultant materials were characterised by XRD, DSC, FT-IR, Raman, UV-Vis, and PL spectroscopy. The materials synthesised ( $T > 400\text{ }^\circ\text{C}$ ) were shown to have a high crystal quality. The silver modification was effective at low temperatures such as  $400 - 600\text{ }^\circ\text{C}$  and results in a reduction of the crystallite size of the 3%-Ag material relative to ZnO. Photocatalytic activity of all samples were determined by analysing the degradation of rhodamine 6G in presence of the powdered suspensions. Silver modification caused the material to show significant improvement in the photocatalytic activity. 3 mol% silver at  $400\text{ }^\circ\text{C}$  was considered as the optimum concentration which shows four times higher rate of degradation of dye than that of unmodified ZnO. The mechanism of photocatalytic activity was studied by analysing the emission properties and it was found that the presence of silver facilitates the interfacial charge transfer processes in such a way to utilise the CB electron for enhancing the

1 photocatalytic activity. This results show that silver has a significant role to play in the trapping of  
2 electrons in these materials, and as such these materials applications could be extend to the development  
3 of a photocatalyst which is applicable in both environmental purification and energy production  
4 processes.  
5  
6  
7  
8  
9

## 10 **Acknowledgements**

11 RG acknowledges HEA Strand I for funding  
12  
13  
14  
15  
16  
17  
18  
19

20 **Supporting Information available:** Table of crystallite sizes for all samples, IR spectra of silver  
21 modified ZnO samples at 300 °C and Table of rate constants of photodegradation of R6G and sunlight  
22 photocatalysis kinetic data. This material is available free of charge via the Internet at  
23 <http://pubs.acs.org>.  
24  
25  
26  
27  
28  
29

## 30 **References**

- 
- 31  
32  
33  
34  
35  
36 1 Afzaal, M.; Malik, M. A.; O'Brien, P. *New J. Chem.* **2007**, 31, 2029  
37  
38 2 Kamat, P.V. *J. Phys. Chem. C* **2007**, 111, 2834. 2029.  
39  
40 3 Mills, A.; Wang, J. *J. Photochem. Photobiol. A: Chem.* **2006**, 182, 181  
41  
42 4 Hoffmann, M. R.; Martin, S. T.; Choi, W.; Bahnemann, D. W. *Chem. Rev.* **1995**, 95,69  
43  
44 5 Vayssieres, L. *Adv. Mater.* **2003**, 15, 464.  
45  
46 6 Periyat, P.; Pillai, S. C.; McCormack, D. E; Colreavy, J., Hinder, S. J. *J. Phys. Chem. C* **2008**, 112, 44.  
47  
48 7 Pang, Z.W.; Dai, Z. R; Wang, Z. L. *Science* **2001**, 291, 1947.  
49  
50 8 Bahadur, L.; Rao, T. N. *J. Photochem. Photobiol. A: Chem.* **1995**, 91, 233.  
51  
52 9 Norris, B. J.; Anderson, J.; Wager, J. F.; Keszler, D. A. *J. Phys. D. Appl. Phys.* **2003**, 36, 105.  
53  
54 10 Lee, J. B.; Lee, H. J.; Seo, S. H.; Park, J. S. *Thin Solid Films* **2001**, 641, 398.  
55  
56 11 Hu, Z.; Chen, S.; Peng, S. *J. Coll. Interface Sci.*, **1996**, 182,457.  
57  
58 12 Pillai, S. C.; Kelly, J. M.; McCormack, D.E.; Raghavendra, R. *J. Mater. Chem.* **2004**, 14, 1572.  
59  
60

- 1  
2  
3  
4  
5  
6  
7  
8  
9  
10  
11  
12  
13  
14  
15  
16  
17  
18  
19  
20  
21  
22  
23  
24  
25  
26  
27  
28  
29  
30  
31  
32  
33  
34  
35  
36  
37  
38  
39  
40  
41  
42  
43  
44  
45  
46  
47  
48  
49  
50  
51  
52  
53  
54  
55  
56  
57  
58  
59  
60
- 13 Pillai, S. C.; Kelly, J. M.; McCormack, D. E.; O'Brien, P.; Raghavendra, R. *J. Mater. Chem.* **2003**, 13, 2586.
- 14 Gouvea, C. A. K.; Wypych, F.; Moraes, S. G.; Duran, N.; Peralta-Zamora, P. *Chemosphere* **2000**, 40, 427.
- 15 Sang, B.; Konagai, M. *J. Appl. Phys.* **1996**, 35, 602.
- 16 Dionysiou, D. D.; Suidan, M. T.; Bekou, E.; Baudin, I.; Laîné, M. J. *Appl. Catal. B: Environ.* **2000** 26, 153.
- 17 Sibin, C. P.; Kumar, S. R.; Mukundan, P.; Warriar, K. G. K. *Chem. Mater.* **2002**, 14, 2876.
- 18 Padmanabhan, S. C.; Pillai, S. C.; Colreavy, J.; Balakrishnan, S.; McCormack, D. E.; Perova, T. S.; Gun'ko, Y.; Hinder, S. J.; Kelly, J. M. *Chem. Mater.* **2007**, 19, 4474.
- 19 Subramanian, V.; Wolf, E.; Kamat, P. V. *J. Phys. Chem. B* **2001**, 105, 11439.
- 20 Pillai, S. C.; Periyat, P.; George, R.; McCormack, D. E.; Seery, M. K.; Hayden, H.; Colreavy, J.; Corr, D.; Hinder, S. J. *J. Phys. Chem. C* **2007**, 111, 1605.
- 21 Asahi, R.; Morikawa, T.; Ohwaki, T.; Aoki, K.; Taga, Y. *Science* **2001**, 13, 269.
- 22 Qui, X.; Li, G.; Sun, X.; Li, L.; Fu, X. *Nanotech.* **2008**, 19, 215703.
- 23 Hariharan, C.; *Appl. Cat. A: Gen.* **2006**, 304, 55.
- 24 Kamat, P. V.; Huehn, R.; Nicolaescu, R.; *J. Phys. Chem. B* **2002**, 106, 788.
- 25 Hermann, J. M.; Tahiri, H.; Ait-ichou, Y.; Lossaletta, G.; Gonzalez-Elipse, A. R.; Fernandez, A. *Appl. Catal. B: Environ.* **1997**, 13, 219.
- 26 Kamat, P. V. *J. Phys. Chem. B* **2002**, 106, 7729.
- 27 Kang, H. S.; Ahn, B. D.; Kim, J. H.; Kim, G. H.; Lim, S. H.; Chang, H. W.; Lee, S. Y. *Appl. Phys. Lett.* **2006**, 88, 202108.
- 28 Pathak, P.; Meziani, M. J.; Castillo, L.; Sun, Y. P. *Green Chem.* **2005**, 7, 667.
- 29 Chao, H. E.; Yun, Y. U.; Xiangfang, H. U.; Larbot, A. *J. Eur. Cer. Soc.* **2003**, 23, 1457.
- 30 Stathatos, E.; Petrova, T.; Lianos, P. *Langmuir* **2001**, 17, 5025.
- 31 Seery, M. K.; George, R.; Floris, P.; Pillai, S. C. *J. Photchem. Photobio. A: Chem.* **2007**, 189 (2-3), 258.
- 32 Hirakawa, T.; Kamat, P. V. *J. Am. Chem. Soc.* **2005**, 127, 3928.
- 33 Wang, R.; Xina, J. H.; Yang, Y.; Liu, H.; Xu, L.; Hu, J. *Appl. Surf. Sci.* **2004**, 227, 312.
- 34 Jeong, S.H.; Park, B.N.; Lee, S. B.; Boo, J. H. *Surf. Coat. Tech.* **2005**, 193, 340.
- 35 Height, M. J.; Pratsinis, S. E.; Mekasuwandumrong, O.; Praserthdam, P. *Appl. Catal. B: Environ.* **2006**, 63, 305.
- 36 Pillai, S. C.; Kelly, J. M.; McCormack, D.E.; Ramesh, R. *Mater. Sci. Tech.* **2004**, 20, 964.



- 1  
2  
3  
4  
5  
6  
7  
8  
9  
10  
11  
12  
13  
14  
15  
16  
17  
18  
19  
20  
21  
22  
23  
24  
25  
26  
27  
28  
29  
30  
31  
32  
33  
34  
35  
36  
37  
38  
39  
40  
41  
42  
43  
44  
45  
46  
47  
48  
49  
50  
51  
52  
53  
54  
55  
56  
57  
58  
59  
60
- 37 Spanhel, L.; Anderson, M.A. *J. Am. Chem. Soc.* **1991**, 113, 2826.
- 38 Ahn, B. D.; Kang, H. S.; Kim, J. H.; Chang, H. W.; Lee, S.Y. *J. Appl. Phys.* **2006**, 100, 093701.
- 39 Fan, J.; Freer, R. *J. Appl. Phys.* **1995**, 77, 9.
- 40 Blinks, D. J.; Grimes, R. W. *J. Am. Ceram. Soc.* **1993**, **76**, 2370.
41. Pillai, S. C.; Kelly, J. M.; McCormack, D.E.; Ramesh, R. *J. Mater. Chem.* **2008**, DOI:10.1039/b804793f.
- 42 Chuang H. J.; Ko, H. W. *Proc. Natl. Sci. Counc., Repub. China A: Phys. Sci. Eng.* **1989**, 13, 145
- 43 Wu, J. J.; Liu, S. C. *J. Phys. Chem. B* **2002**, 106, 9546.
- 44 Aarthi, T.; Madras, G. *Ind. Eng. Chem. Res.* **2007**, 46, 7.
- 45 Qiu Y.; Zhang, F; Zhao, F; Tang Y.; Song X. *J. Photochem. Photobiol.* **1995**, 85(3), 281.
- 46 Hermann, J. M.; Disdier, J.; Pichat, P. *J. Phys. Chem.* **1986**, 90, 6028.
- 47 Sclafani, A.; Hermann, J. M. *J. Photochem. Photobiol. A* **1998**, 113, 181.
- 48 Kuo, S.T.; Tuan, W.H.; Shieha, J.; Wang, S.F. *J. Eur. Ceram. Soc.* **2007**, 27, 4521.
- 49 Yang, Q.J.; Choi, H.; Dionsyiou, D. D. *Appl. Cat. B: Environ.* **2007**, 74, 170.
- 50 Zhang, L.; Yu.; J. C.; Yip H. Y.; Li, Q.; Kwong, K.W.; Xu, A.W.; Wong, P.K. *Langmuir* **2003**, 19, 10372.
- 51 Vanheusden, K.; Warren, W. L.; Seager, C. H.; Tallant, D. R.; Voigt, J. A. *J. Appl. Phys.* **1996**, 79, 7983.
- 52 Djuricic, A.B.; Leung, Y.H.; Choy, C. W. C. H.; Cheah, K.W.; Chan, W.K. *Appl. Phys. Lett.* **2004**, 84, 2635.
- 53 Kamat; P. V.; Patrick, B. *J. Phys. Chem.* **1992**, 96, 6829.
- 54 Manticone, S.; Tefeu, R.; Kanaev, A.V. *J. Phys. Chem. B* **1998**, 102, 2854.
- 55 Yao, B.D.; Chan, Y.F.; Wang, N. *Appl. Phys. Lett.* **2002**, 81, 757.
- 56 Subramanian, V.; Wolf, E. E.; Kamat, P.V. *J. Phys. Chem. B* **2003**, 107, 7479.
- 57 Wang, X.; Li, Q.; Liu, Z.; Zhang, J.; Liu, Z. *Appl. Phys. Lett.* **2004**, 84, 4941.
- 58 Kanai, Y. *J. Appl. Phys.* **1991**, 30, 2021.
- 59 Waterhouse, G. I. N.; Bowmaker, G. A.; Metson, J. B. *Phys. Chem. Chem. Phys.* **2001**, 3, 3838
- 60 L'Vov, B. V. *Thermochim. Acta* **1999**, 13, 333.
- 61 Dallek, S.; Larrick, B. F.; West, W. A. *J. Electrochem. Soc.* **1986**, 133, 245.
- 62 Dodd, A.C.; Mckinley, A.J.; Saunders, M.; Tsuzuki, T. *J. Nano. Research* **2006**, 8, 43.

1  
2  
3  
4  
5  
6  
7  
8  
9  
10  
11  
12  
13  
14  
15  
16  
17  
18  
19  
20  
21  
22  
23  
24  
25  
26  
27  
28  
29  
30  
31  
32  
33  
34  
35  
36  
37  
38  
39  
40  
41  
42  
43  
44  
45  
46  
47  
48  
49  
50  
51  
52  
53  
54  
55  
56  
57  
58  
59  
60

63 Bahnemann, D. *Solar Energy* 2004, 77, 445.

64 Jing, L.Q.; Qu, Y.; Wang, B.; Li, S.; Jiang, B.; Yang, L.; Wei, F.; Fu, H. *J. Sun, Solar Ener. Mater. Solar Cells* **2006**, 90, 1773

65 Zhou, Z.; Quian, S.; Yao, S. Zhang, Z. *Rad. Phys. Chem.* **2002**, 65, 241.

66 Zhao, J.; Wu,; Wu, T. K.; Oikawa, K.; Hidaka, H.; Serpon, N. *Environ. Sci. Tech.* **1998**, 32, 2394.

67 Bandara, J.; Tennakone, K.; Binduhewa, P. *New J. Chem.* **2001**, 25, 1302.

68 Liu, S.X.; Qu, Z.P.; Han, X. W.; Sun, C. L. *Catalysis Today* **2004**, 93, 877.

69 Kamat, P.V. *Pure Appl. Chem.* **2002**, 74, 1693.

70 Jakob, M.; Levanon, H.; Kamat, P.V. *Nanoletters* **2003**, 3, 353.